



HAL
open science

Mediterranean mussels (*Mytilus galloprovincialis*) exposure to fluoxetine: Bioaccumulation and biotransformation products

Etienne Lemaire, Elena Gomez, Nicolas Le Yondre, Amélie Malherbe, F
Courant

► To cite this version:

Etienne Lemaire, Elena Gomez, Nicolas Le Yondre, Amélie Malherbe, F Courant. Mediterranean mussels (*Mytilus galloprovincialis*) exposure to fluoxetine: Bioaccumulation and biotransformation products. *Chemosphere*, 2024, 365, pp.143314. 10.1016/j.chemosphere.2024.143314 . hal-04711576

HAL Id: hal-04711576

<https://hal.science/hal-04711576v1>

Submitted on 27 Sep 2024

HAL is a multi-disciplinary open access archive for the deposit and dissemination of scientific research documents, whether they are published or not. The documents may come from teaching and research institutions in France or abroad, or from public or private research centers.

L'archive ouverte pluridisciplinaire **HAL**, est destinée au dépôt et à la diffusion de documents scientifiques de niveau recherche, publiés ou non, émanant des établissements d'enseignement et de recherche français ou étrangers, des laboratoires publics ou privés.



Distributed under a Creative Commons Attribution 4.0 International License



Mediterranean mussels (*Mytilus galloprovincialis*) exposure to fluoxetine: Bioaccumulation and biotransformation products

E. Lemaire^a, E. Gomez^{a,c}, N. Le Yondre^b, A. Malherbe^a, F. Courant^{a,c,*}

^a Hydrosiences Montpellier, University of Montpellier, CNRS, IRD, Montpellier, France

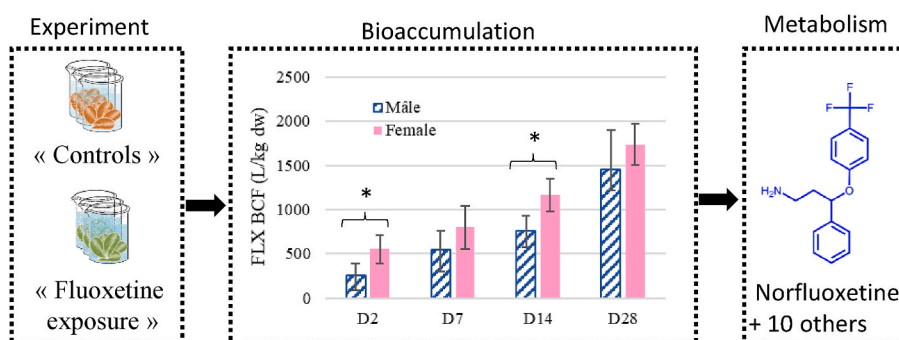
^b Univ. Rennes, CNRS, Centre Régional de Mesures Physiques de l'Ouest (CRMPO), UAR 2025 ScanMAT, F-35042, Rennes, France

^c Montpellier Alliance for Metabolomics and Metabolism Analysis, Platform on non-target exposomics and metabolomics (PONTEM), Biocampus, CNRS, INSERM, Université de Montpellier, Montpellier, France

HIGHLIGHTS

- FLX uptake by mussels was rapid.
- A 28-day FLX exposure confirms continuous bioaccumulation in mussel.
- Males and females accumulated FLX differently at the beginning of the exposure.
- Eleven FLX metabolites were highlighted using an MS-based non-targeted approach.
- Ten FLX metabolites are reported for the first time in *Mytilus galloprovincialis*.

GRAPHICAL ABSTRACT



ARTICLE INFO

Handling editor: Keith Maruya

Keywords:

Bioaccumulation
Biotransformation
Metabolites
Mussels
Mass spectrometry
Pharmaceuticals

ABSTRACT

The significant rise in antidepressant consumption in recent years was accentuated by COVID-19 pandemic. Among these antidepressants, fluoxetine, a selective serotonin re-uptake inhibitor (SSRI), is the most prescribed worldwide. The present study investigated its bioaccumulation and metabolization in the mussel *Mytilus galloprovincialis*, generally recognized as a reliable bioindicator for assessing environmental quality and the accumulation of various contaminants. Mussels were exposed to a nominal concentration of fluoxetine (3.1 µg/L) for 28 days. Mussels were sacrificed at day 2, 7, 14 and 28 of exposure. The order of accumulation level was gills > digestive glands > soft tissues, and a regular increase in fluoxetine and norfluoxetine was observed across the various sampling days for both digestive glands and soft tissues. The calculated bioconcentration factor (BCF) ranged from 253 at D2 to 1734 at D28 for fluoxetine, and pseudo-BCF from 7 at D2 to 64 at D28 for norfluoxetine. Non-targeted approaches highlighted ten metabolites, which are reported for the first time in *Mytilus*, in addition to norfluoxetine. Notably, this study highlighted two phase I metabolites and one phase II metabolite previously unreported. These findings contribute to the understanding of fluoxetine accumulation and metabolism in *Mytilus* and enhance the knowledge of pharmaceuticals detoxification processes in non-target organisms.

* Corresponding author. HydroSciences Montpellier, IRD, CNRS, University of Montpellier, 15 avenue Charles Flahault, 34093 Montpellier, France.

E-mail address: frederique.courant@umontpellier.fr (F. Courant).

<https://doi.org/10.1016/j.chemosphere.2024.143314>

Received 17 July 2024; Received in revised form 6 September 2024; Accepted 9 September 2024

Available online 13 September 2024

0045-6535/© 2024 The Author(s). Published by Elsevier Ltd. This is an open access article under the CC BY license (<http://creativecommons.org/licenses/by/4.0/>).

1. Introduction

The consumption of antidepressants has seen a significant rise over recent years, a trend that has been further accentuated by the COVID-19 pandemic, more than twice (OECD, 2019; Diaz-Camal et al., 2022). Among the various antidepressants available, fluoxetine (FLX), commonly known by its brand name Prozac, stands out as the most prescribed worldwide. Its release through wastewater treatment plant effluents heavily impacts aquatic environments (Verlicchi et al., 2012) and have raised concerns, particularly regarding its presence in marine ecosystems. FLX is frequently detected in estuarine and coastal water around the world, at concentrations ranging from 1.09 ng/L to 16.2 ng/L in Portugal (Reis-Santos et al., 2018), up to 36 ng/L in an Australian estuary (Birch et al., 2015), from non-detectable (n.d.) to 0.6 ng/L in Spain (Biel-Maeso et al., 2018) and from n.d. to 41 ng/L in Mahdia coastal waters (Tunisia) (Afsa et al., 2020). In the ocean, reported concentrations range from n.d. to 1.6 ng/L in oceanic waters from the Gulf of Cadiz in Spain (Biel-Maeso et al., 2018) and to higher concentrations at 90 ng/L in the Pacific Ocean (USA) (Nödler et al., 2014). FLX not only persists in the marine water but also tends to accumulate in non-target marine organisms (Silva et al., 2015), such as sponges (Rizzi et al., 2020), or mussels (Silva et al., 2017; Maruya et al., 2012). Mussels are frequently subjected to such exposure and a mean concentration of FLX of 4.83 µg/kg was reported from 9 different locations along the Portugal Atlantic coast (Silva et al., 2017). While some information exists about the bioaccumulation of various pollutants, specific data on fluoxetine remain limited (Boxall et al., 2012; Franzellitti et al., 2014).

Mussels play a crucial role in environmental biomonitoring endeavors as sedentary organisms with a broad geographic range and a high tolerance for environmental fluctuations (Boening, 1999; Regoli and Principato, 1995). The genus *Mytilus* is generally recognized as a reliable bioindicator for assessing environmental quality and the accumulation of various contaminants (Gaitán-Espitia et al., 2016). Indeed, as filter feeders, they intake water and particles from their surroundings (Cranford et al., 2011). Due to these characteristics, *Mytilus* is considered an ideal organism for studying the bioaccumulation of fluoxetine. Understanding this process can provide valuable insights into both environmental and human health, since mussels are intended for human consumption. The exposure of mussels to FLX can lead to effects such as an increase in foot size, resulting in an inability to close shell (Bringolf et al., 2010), impaired regulation of spawning (Fong et al., 1994) and behavioral changes such as an increased activity rate, reducing the filtering function in species like *Mytilus californianus* (Hazelton et al., 2014).

It seems also essential to study the relationship between bioaccumulation and metabolism for this molecule as detoxification mechanisms may mitigate its effects. Several studies have investigated the metabolism of pharmaceutical products in mussels (Ariza-Castro et al., 2021; Bonnefille et al., 2017). Parent pharmaceutical compounds typically undergo biotransformation to generate other compounds, some of which may exhibit varying degrees of activity compared to the parent compound. In the case of FLX, numerous studies have focused on its primary metabolite, norfluoxetine (NFLX), which has been found to be as pharmacologically active than FLX itself (Claesson and Svensson, 1996). However, limited research has been conducted on the study of other FLX metabolites formed in aquatic organisms. The study of its biotransformation in zebrafish embryos, revealed metabolic pathways such as N-demethylation, hydroxylation, or N-acylation (Tisler et al., 2019; Zindler et al., 2020). To the best of our knowledge, only one other study has observed different FLX metabolites than NFLX in freshwater organisms, i.e. microalgae (Xie et al., 2022). Moreover, the equilibrium between absorption and excretion, including the role of biotransformation processes over medium to long-term periods, remains poorly understood. Most existing studies are short-term, often lasting less than 15 days, limiting the understanding of fluoxetine's behavior in marine organisms over extended periods (Franzellitti et al., 2014; Silva et al.,

2016).

Given these knowledge gaps, our study aims to address these critical issues by investigating the bioaccumulation and biotransformation of fluoxetine in mussels, thus contributing to the broader field of ecotoxicology. To this end, *Mytilus galloprovincialis* were exposed to a FLX concentration of 3.1 µg/L for 28 days. Using a mass spectrometry-based targeted approach, the levels of FLX and its primary metabolite NFLX were measured in various tissues (gills, digestive gland, and soft tissues) to examine their distribution and accumulation over time. Additionally, a mass spectrometry-based targeted and non-targeted approach was conducted on digestive glands to screen for already known (based on literature) FLX metabolites, and to identify any potential FLX metabolites not previously documented which would be generated by Mediterranean mussels after exposure.

2. Material and methods

2.1. Chemicals

The analytical standard of fluoxetine hydrochloride (FLX) and fluoxetine-d₆ (FLX-d₆) were purchased from Sigma-Aldrich (Steinheim, Germany). Norfluoxetine hydrochloride (NFLX), 4-(trifluoromethyl)-phenol (TFMP) and norfluoxetine-d₅ hydrochloride (NFLX-d₅) were acquired from Santa Cruz Biotechnology (Texas, USA). N-formyl-fluoxetine (N-formylFLX) was purchased from Toronto Research Chemicals (Toronto, Canada). All standards were purchased at analytical grade (purity >98%). Stock standard solutions of each compound were prepared in methanol at a concentration of 1 mg/mL. All the standard solutions were stored at -20 °C. A working standard solution for each standard was prepared at concentration of 1 µg/mL in methanol. Ultrapure water was generated by a Millipore Milli-Q system (Milford, MA, USA). Methanol (MeOH), and HPLC-grade acetonitrile (ACN) were obtained by Carlo Erba (Val de Reuil, France). Formic acid (FA) (purity, 98%) was supplied from Fisher Scientific Labosi (Elancourt, France). Solid phase extraction (SPE) Oasis HLB™ cartridge (200 mg, 6 cc) was purchased from Waters, (Milford, MA, USA), Phree™ phospholipid removal (1 mL) was acquired from Phenomenex (Torrance, CA, USA). Nanosep® centrifugal filters 0.2 µm were purchased from Pall Corporation (Port Washington, NY, USA). The seawater was collected at the IFREMER station in Palavas-Les-Flots, France. Subsequently, it underwent sterilization through UV treatment and degassing following filtration with a sand filter.

2.2. Animals and fluoxetine exposure experiment

Mytilus galloprovincialis mussels were purchased in February from a Mediterranean mussel supplier (Bouzigues, France) and immediately transported to the laboratory (<1 h). After they were cleaned, the mussels were acclimatized in aerated (9 mg/L) filtered (GF/F, Whatman) natural seawater (salinity of 55 g/L, pH = 7.9) for 7 days before the experiment. During the acclimation and exposure periods, seawater was renewed every two or three days (semi-static renewal) and water temperature was regulated at 15.4 ± 0.8 °C. Mussels were fed daily, 1 h before FLX concentration spiking, with *Tetraselmis suecica* (Greensea, Mèze, France) at constant density (20,000 cells/mL). After acclimatization, 240 individuals (shell length 7–8 cm) were randomly allocated in 24 glass aquaria, each with a volume of 4-liter seawater, at a density of 2.5 mussels per liter. Two groups were formed consisting of 12 glass aquaria each: a solvent control (SC) group and an exposed (E) group exposed to a nominal concentration of 3.1 µg/L of FLX. During the exposure period of 28 days (4 weeks), FLX concentrations were re-established after each water renewal. Seawater (10 mL) was sampled once a week, FLX concentration was followed over 48h. Sampling (10 mL) was conducted after water renewal and spiking at t = 0 + 15 min, then every hour during the day, and finally at t = 24 h and t = 48 h. Water samples were spiked with 31 ng of deuterated internal standards (FLX-

d₆) before freezing (−20 °C). Triplicate aquaria without mussels were used as well to assess glass adsorption, with concentration measurements taken at zero, 24, and 48 h. Mussels (3 aquaria of 10 mussels each from both conditions) were sampled at 2, 7, 14 and 28 days (Figure S-1). Mussels were dissected: gills, digestive glands and the remaining soft tissues were frozen at −80 °C before freeze drying during five days (Heto Power dry LL 3000, Thermo) and analysis. Sex of mussels was determined by microscopic analysis of a gonadal smear. After 28 days of exposure, mussel mortality was below 3% in agreement with the Organization for Economic Co-Operation and Development (OECD) guidelines.

2.3. Sample preparation

2.3.1. Seawater

The extraction of FLX from seawater was performed by SPE cartridges Oasis HLB (200 mg, 6 cc). Cartridges were first conditioned with 6 mL of methanol followed by 6 mL of water. Afterwards, samples (10 mL) were loaded onto cartridges. After a drying step of 3 min, the latter were cleaned with 6 mL of a mixture water/methanol (v/v, 90/10). After a second drying step of 15 min, elution of FLX was completed twice with 5 mL of methanol. Finally, eluates were evaporated to dryness under a nitrogen stream and re-suspended in 100 µL of water/acetonitrile (v/v, 80/20). An extracted calibration curve with blank seawater samples spiked at 0, 0.1, 0.5, 1, 2 and 5 µg/L with FLX and 3.1 µg/L FLX-d₆ was prepared in the same way for quantification purposes.

2.3.2. Tissues

Before analysis, the freeze-dried samples (gills, digestive glands and the remaining soft tissues) were ground in a ball mill (Retsch MM400) to ensure homogenization.

Regarding soft tissues, analysis of FLX and its metabolites was conducted from 400 mg dry tissues, which were spiked with 40 ng of FLX-d₆ and 4 ng NFLX-d₅ surrogate standards (corresponding to concentrations of 100 µg/kg and 10 µg/kg, respectively) and extracted twice using 10 mL of acetonitrile (ACN) containing 0.1% formic acid. Pooled supernatants were collected and concentrated to 2 mL and passed through a solid-phase extraction (SPE) Phree™ phospholipid removal cartridge, previously conditioned with 0.5 mL of ACN. Following the addition of 2 mL of ACN on the cartridge, eluates were evaporated to dryness under a gentle stream of nitrogen at 40 °C. Finally, dried extracts were reconstituted in 200 µL of ACN/water (v/v, 20/80) and filtered through Nanosep® centrifugal filters with a pore size of 0.2 µm. To perform quantification, an extracted calibration curve was prepared in the same way with soft-tissue samples spiked at 0, 200, 500, 1000, 2000, 3500 and 5000 µg/kg of FLX and 0, 1, 5, 10, 20, 50 and 100 µg/kg for its metabolite NFLX.

For gills and digestive glands, 40 mg of dry tissues were used. After spiking with 4 ng of FLX-d₆ and NFLX-d₅ surrogate standards (corresponding to concentrations of 100 µg/kg), samples were extracted twice with 1 mL of ACN containing 0.1% formic acid. Pooled supernatant were then passed through an SPE Phree™ phospholipid removal cartridge, previously conditioned with 0.5 mL of ACN. The final steps were similar to the extraction process for soft tissues. To conduct quantification, extracted calibration curves were prepared in a similar manner using gills and digestive glands samples spiked at concentrations of 0, 500, 2000, 3500, 5000, and 10000 µg/kg of FLX and 0, 50, 100, 250, 500, 1000 and 2500 µg/kg for its metabolite NFLX.

2.4. HPLC-Orbitrap MS analysis

2.4.1. Quantification of FLX/NFLX

Separation of analytes was performed using an HPLC Vanquish HPLC (ThermoFisher Scientific, Bremen, Germany) equipped with a modified C18 analytical column, 100 mm length × 2.1 mm i.d. and 2.6 µm particle size (Kinetex biphenyl, Phenomenex, Torrance, CA, USA). The

temperature of column oven was set at 28 °C and the autosampler chamber at 4 °C. The mobile phase was constituted of water (A) and ACN (B) both modified with 0.1% formic acid and used at flow rate of 300 µL/min. The volume of injection was 10 µL. Initial condition (20% B) were maintained for 1 min, before the percentage of the organic phase (B) was increased from 20% to 60% at 3 min. The organic phase (B) increased again to 100% B at 6 min. Then, the organic phase was maintained for 4 min at 100% B before returning to the initial conditions in 2 min (reequilibration for the next 6 min). This gradient provided an 18-min chromatographic run.

For the analysis, an Orbitrap Exploris 240 HRMS (ThermoFisher Scientific, Bremen, Germany) system equipped with a heated electrospray ionization source (HESI) operating in positive ion mode was used. The HESI parameters were: 4 kV for electrospray voltage; 40 for sheath gas (arbitrary units); 10 for auxiliary gas (arbitrary units); 150 °C heater temperature; 300 °C capillary temperature. Data acquisition involved continuous alternation between full scan and MS² product ion scan modes, both ranging from *m/z* 100 to 700. For product ion scan mode, a high-energy collision dissociation (HCD) cell was used. The mass resolution was 30,000 FWHM for full scan and 15,000 FWHM for product ion scan. The acquisition parameters for FLX and NFLX quantification are presented in supplementary data (Figure S-2). For quantification purposes the transition *m/z* 310.1 → 148.1122 (*m/z* 316.1 → 154.1496) and *m/z* 296.1 → 134.0964 (*m/z* 301.1 → 139.1277) were used for FLX (FLX-d₆) and NFLX (NFLX-d₅), respectively.

2.4.2. Non targeted analysis of FLX metabolites in digestive glands

Chemical profiles of digestive glands from control and FLX exposed mussels at days 2, 7, 14 and 28 (4/control and 10/exposed, half male and half female for each day) were generated by LC-HRMS. The chromatographic parameters were similar to the method used for quantifying FLX and NFLX.

Regarding data acquisition by mass spectrometry, a full scan was performed in both positive and negative modes, with a range from *m/z* 60 to 850. In positive and negative mode, the electrospray voltage was set at 3.35 kV, and the mass resolution at 11,250 FWHM. The other parameters of the HESI method, including sheath gas, auxiliary gas, heater temperature, and capillary temperature, remained unchanged compared to the FLX and NFLX quantification method.

2.4.3. MS/MS confirmation of FLX metabolites

The chromatographic column, mobile phase, flow rate, and HESI source parameters were similar to those described in 2.4.2. However, another gradient was implemented to improve chromatographic separation of FLX metabolites. The initial condition (30% B) was maintained for 2 min, after which the percentage of the organic phase (B) was increased to 55% at 4.5 min. This concentration of the organic phase (B) was sustained for 1.5 min and then raised to 75% B at 7 min. After maintaining 75% B for 2 min, the organic phase was further increased to 100% B at 10 min and held for 3 min before returning to the initial conditions over a period of 4 min. This gradient allowed for a 17-min chromatographic run. Data acquisition involved product ion scan mode, and a high-energy collision dissociation (HCD) cell was used with collision energy adapted for each metabolite. The mass resolution was set at 15,000 FWHM. The new retention times of each highlighted metabolite are reported in Table 2 and Figure S-3 to S-4 along with their fragmentation spectra in Figure S-6 to Figure S-43.

2.5. Method performances for FLX and NFLX

The method performances for each matrix were evaluated by considering various aspects, including linearity, limit of detection (LOD) and quantification (LOQ) of the methods, absolute recovery, matrix effects and repeatability per analyte. Linearity was evaluated using the square correlation coefficient (R²) and determined through calibration curves in solvent and tissues at six different levels. The LOQ was

determined as the minimum concentration for which the difference between the theoretical concentration and the calculated concentration was less than 20%. The limit of detection (LOD) was established as the minimum concentration value below the LOQ, where a chromatographic peak could be detected ($S/N > 3$). In case where the LOQ was already the lowest concentration in the calibration curve, the LOD was calculated as the third of LOQ. Absolute recoveries, matrix effects and repeatability of the methods were evaluated by spiking triplicate blank tissues (3 before and 3 after purification procedure) with 100 $\mu\text{g}/\text{kg}$ (dw) of FLX, FLX-d₆, NFLX and NFLX-d₅ for soft tissues, 200 $\mu\text{g}/\text{kg}$ (dw) of each native and internal standards for gills and digestive gland and triplicate seawater with 3.1 $\mu\text{g}/\text{L}$ of FLX and FLX-d₆. Absolute recoveries were assessed by comparing the signal area of each analyte in blank tissue samples spiked before and after the extraction/purification process, both injected under the same analytical conditions. Relative recoveries were calculated as the ratio of the absolute recovery of each target compound to that of its internal standard. For repeatability, the relative standard deviation (RSD) was calculated on absolute recoveries by dividing the standard deviation by the mean. Matrix effects were evaluated by comparing the signal area of each analyte in blank tissue samples spiked after extraction/purification with the signal area of each analyte measured in a pure standard injected under the same analytical conditions. The obtained performances are reported in Table 1.

2.6. Data processing and FLX metabolite identification strategy

The presence of FLX metabolites in mussel digestive glands was evaluated through both a non-targeted approach, as detailed below, and a suspect screening approach based on metabolites already reported in the literature. Raw data were converted into mzXML files with MSConvert freeware (ProteoWizard 3.0 (Holman et al., 2014)). ESI+

Elemental compositions of unknown metabolites were generated by the Thermo Xcalibur Qual Browser software (XCalibur 4.2.47), and those with the most suitable C, H, N, O and F compositions, based on the FLX composition, were reported. Confidence levels for metabolite identification were proposed according to (Schymanski et al., 2014). Level 1 corresponds to structures confirmed by the analytical standard injection in the same conditions as samples and based on MS, MS/MS and retention time matching. Level 2 refers to probable structures, proposed based on evidence from the literature or library spectrum data (2a), or on diagnostic MS/MS fragments and/or ionization behavior, parent compound information and the experimental context, in the absence of previously reported information (2b). Level 3 is a tentative candidate with an uncertain exact structure. Level 4 describes compounds for which an unequivocal formula is proposed based on spectral information, while level 5 describes those where only the exact mass (m/z) is available.

2.7. Bioconcentration factor (BCF)

Bioconcentration was evaluated in mussels' whole body at each sampling time. The BCF was typically determined using the following equation (1):

$$BCF = C_b / C_w \quad (1)$$

Where C_b is the concentration of chemical in the biota corresponding to concentration of FLX in mussels' entire body ($\mu\text{g}/\text{kg}$ dw) and C_w ($\mu\text{g}/\text{L}$) is the concentration in seawater. The value used for FLX concentration in water was the target nominal concentration (3.1 $\mu\text{g}/\text{L}$). To obtain C_b , the quantity of FLX (in μg) in each organ (gills, digestive glands, and remaining soft tissues) was calculated using equation (2):

$$FLX \text{ in organ } (\mu\text{g}) = FLX \text{ concentration in organ } (\mu\text{g} / \text{kg dw}) \times \text{organ dry weight (kg dw)} \quad (2)$$

and ESI- acquisitions were processed separately using the XCMS package (Smith et al., 2006) in the R environment to integrate the chromatographic peaks in all samples. This multi-step strategy has already been described by (Ariza-Castro et al., 2021; Bonnefille et al., 2017). XCMS parameters were configured as follows: the m/z interval was set at 0.01 and ppm variation at 5, the signal to noise ratio threshold at 10, the group bandwidth at 8, and the minimum fraction at 0.5. After data processing, XCMS generated a table containing peak information and peak abundances per sample. Peaks detected exclusively in exposed samples (absent in control samples) and found in at least five replicates among the ten exposed mussels were considered potential FLX metabolites. Extracted ion chromatograms (EICs) were also processed by Thermo Freestyle 1.5 to confirm the absence of signal in the controls.

C_b ($\mu\text{g}/\text{kg}$ dw) was then determined by dividing the summation of the quantities in each organ (in μg) by the mussels' whole-body weight (in kg, dry weight), using equation (3):

$$C_b = \frac{\sum \text{quantity in organs}}{\sum \text{organs dry weight}} \quad (3)$$

Since the major metabolite NFLX was also detected, the pseudo-bioconcentration factor (pseudo-BCF) was also calculated (i.e., the denominator is the concentration of fluoxetine in the aqueous phase and not the concentration of NFLX), as outlined in previous studies (Nakamura et al., 2008; Paterson and Metcalfe, 2008).

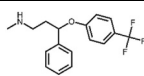
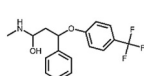
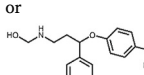
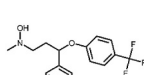
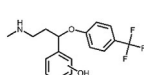
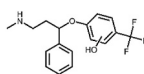
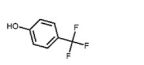
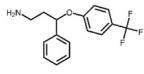
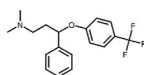
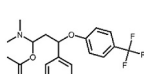
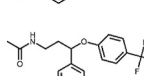
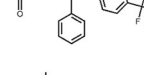
Table 1

Linearity, method detection limit (MDL) and method quantification limit (MQL), matrix effects (ME), and recoveries observed for each FLX and NFLX in water, gills, digestive glands and soft tissues.

Matrix	Analyte	Linear range ($\mu\text{g}/\text{kg}$)	Matrix matched linearity (R^2)	MDL ($\mu\text{g}/\text{kg}$)	MQL ($\mu\text{g}/\text{kg}$)	ME (%)	Absolute recovery (%)	Relative recovery (%)	RSD (%)
Digestive glands	Fluoxetine	0-10,000	0.9969	5.2	10.6	-64	70	102	4
	Norfluoxetine	0-2500	0.9989	24.9	51.3	-50	50	88	7
Gills	Fluoxetine	0-10,000	0.9966	1.0	5.1	-52	91	99	6
	Norfluoxetine	0-2500	0.9942	24.9	50.4	-31	72	89	4
Soft tissue	Fluoxetine	0-5000	0.9985	0.5	1.1	-51	47	92	1
	Norfluoxetine	0-100	0.9976	1.0	5.2	-52	36	90	7
Water	Fluoxetine	0-5	0.9963	0.05	0.1	-92	69	91	17

Table 2

Summary of FLX and its metabolites detected in mussel digestive gland. Retention time (min), observed molecular ion ($[M+H]^+$ or $[M-H]^-$), structure, confidence level based on Schimanski et al. (2014) and relevant references that already reported the metabolite in aquatic organisms.

Peak ID	rt (min)	Assignment	Elemental composition [M]	Ionization mode	Observed $[M+H]^+$ or $[M-H]^-$ (δ ppm)	Structure	Confidence level ^a	Relative abundance ^b	References
P	4.41	FLX	C ₁₇ H ₁₈ F ₃ NO	+	310.1414 (0.30 ppm)		1	++++	
M1	2.45	HydroxyFLX (a)	C ₁₇ H ₁₈ F ₃ NO ₂	+	326.1367 (1.56 ppm)		2b	++	
M2	3.06	HydroxyFLX (b)	C ₁₇ H ₁₈ F ₃ NO ₂	+	326.1367 (1.56 ppm)	or  	2a	+	Second structure proposal: Tisler et al., 2019 Xie et al., 2022 Yan et al., 2023 Zindler et al., 2020
M3	3.39	HydroxyFLX (c)	C ₁₇ H ₁₈ F ₃ NO ₂	+	326.1367 (1.56 ppm)		2b	++	Zhao et al., 2017 Tisler et al., 2019 Yan et al., 2023 Zindler et al., 2020
M4	3.47	HydroxyFLX (d)	C ₁₇ H ₁₈ F ₃ NO ₂	+	326.1367 (1.56 ppm)		2b		
M5	3.95	4-(trifluoromethyl)phenol (TFMP)	C ₇ H ₅ F ₃ O	-	161.0221		1	++	Tisler et al., 2019 Xie et al., 2022 Yan et al., 2023
M6	4.07	NFLX	C ₁₆ H ₁₆ F ₃ NO	+	296.1260 (1.02 ppm)		1	++	Xie et al., 2022 Zindler et al., 2020
M7	4.67	MethylFLX	C ₁₈ H ₂₀ F ₃ NO	+	324.1576 (2.00 ppm)		2a	++	Zindler et al., 2020
M8	4.69	N-Methyl-AcetoxyFLX	C ₂₀ H ₂₂ F ₃ NO ₃	+/-	382.1631 (1.69 ppm) 380.1479 (1.25 ppm)		2b	+++ / ++	
M9	6.74	N-formylFLX	C ₁₈ H ₁₈ F ₃ NO ₂	+	338.1369 (1.96 ppm)		1	++	Tisler et al., 2019 Xie et al., 2022 Yan et al., 2023
M10	6.79	N-AcetylFLX	C ₁₉ H ₂₀ F ₃ NO ₂	+	352.1505 (3.91 ppm)		2a	++	Tisler et al., 2019 Yan et al., 2023
M11	6.95	N-acrylFLX	C ₂₀ H ₂₀ F ₃ NO ₂	+	364.1528 (2.42 ppm)		2a	++	Tisler et al., 2019 Zindler et al., 2020

^a Based on Schymanski et al. (2014).

^b Relative signal abundance ++++ peak intensity (I) > 1.0E9; +++ I > 1.0E7; ++ I > 1.0E6; + I > 5.0E5.

2.8. Statistics

Statistical differences in FLX and NFLX concentrations between sampling time and across gender for each day were assessed using the Mann-Whitney *U* test. Significant differences were identified using a criterion of a *p* < 0.05. All the data were analyzed using the R studio software (4.2.2 version).

3. Results

3.1. Analysis of FLX in exposure seawater

The analysis of FLX in aquaria without mussels was conducted to verify the absence of glass adsorption. On a two days' period, a significant decrease of FLX concentration was observed (*p*-value = 0.04),

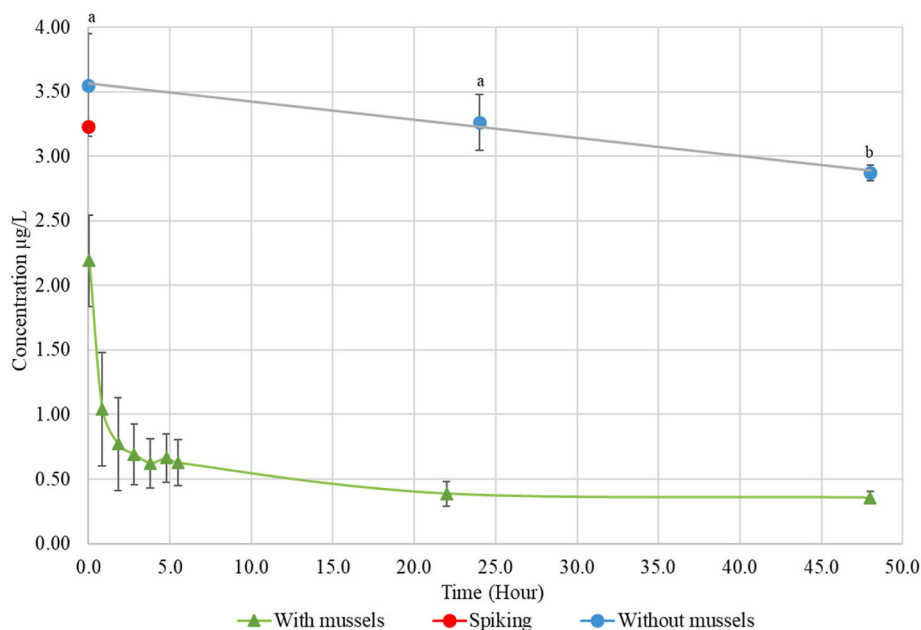


Fig. 1. Average FLX concentration ($\mu\text{g/L}$) measured in water in aquaria without mussels ($n = 3$) (in blue) at $t = 0, 24$ and 48 h and in 3 exposed aquaria during day 16 (in black). The different letters indicate significant differences ($p < 0.05$) between each sampling time in aquaria without mussels. (For interpretation of the references to colour in this figure legend, the reader is referred to the Web version of this article.)

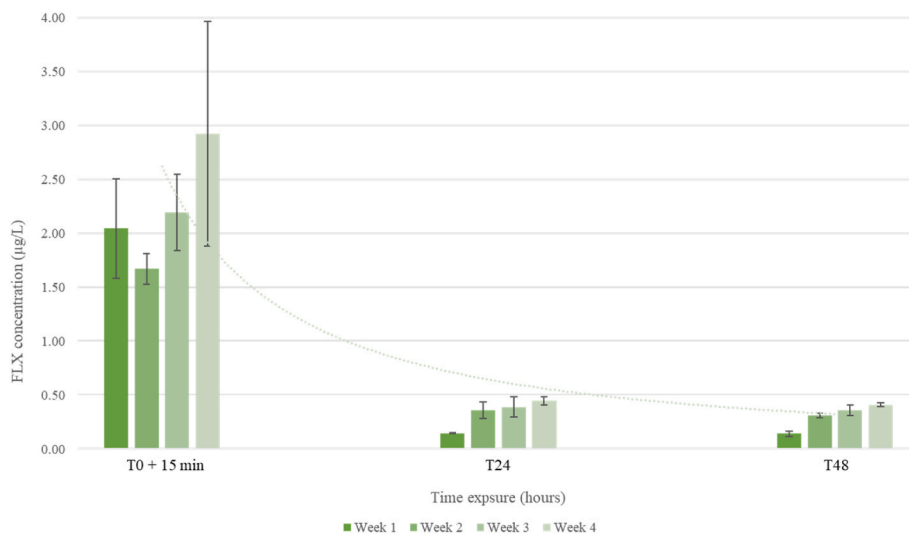


Fig. 2. Variation of FLX concentrations measured in water ($\mu\text{g/L}$) in 3 exposed aquaria during a 48-h period (for 4 spiking cycles). Exposure water samples were collected at 15 min, 24 h, and 48 h after the doping renewal at the beginning of each week.

although less than 20% (Fig. 1). The average measured concentration during this two-day period was $3.2 \mu\text{g/L}$. The difference between the nominal concentration and the measured concentration in the aquaria was less than 20%. Therefore, for the various calculations conducted in this study, the value of $3.1 \mu\text{g/L}$ was retained (OECD guidelines).

The FLX concentrations measured in three aquaria containing mussel for 24 h, depicted a rapid decrease immediately after the addition of the substance. Specifically, within the first 15 min post-addition, the concentration of FLX dropped from an assumed nominal concentration of $3.1 \mu\text{g/L}$ to $2.2 \mu\text{g/L}$ (Fig. 1). FLX concentrations continued to decrease during the first hours and tended towards a limit value around $0.4 \mu\text{g/L}$ at 24 h and 48 h. The same pattern was observed each week (for 4 measured spiking cycles) (Fig. 2). No signal of the parent compound (FLX) was detected in the control aquaria water samples, and there was no signal of the main metabolite NFLX detected in either the control or

exposure water.

Regarding the behavior of FLX in aquaria without and with mussels, it is then possible to hypothesize that FLX was rapidly absorbed by *Mytilus galloprovincialis*, and this throughout the entire exposure experiment. This hypothesis has been confirmed with the quantification of FLX in the various collected organs.

3.2. Analysis of FLX in organs

3.2.1. FLX quantification and distribution in different tissues

The digestive glands, gills, and soft tissues were collected after 2, 7, 14, and 28 days of exposure. Fig. 3 illustrates the tissue concentrations measured for FLX (A) and NFLX (B) across different tissues and sampling days. Nor FLX or NFLX were detected in digestive glands, gills and soft tissues of the control mussels.

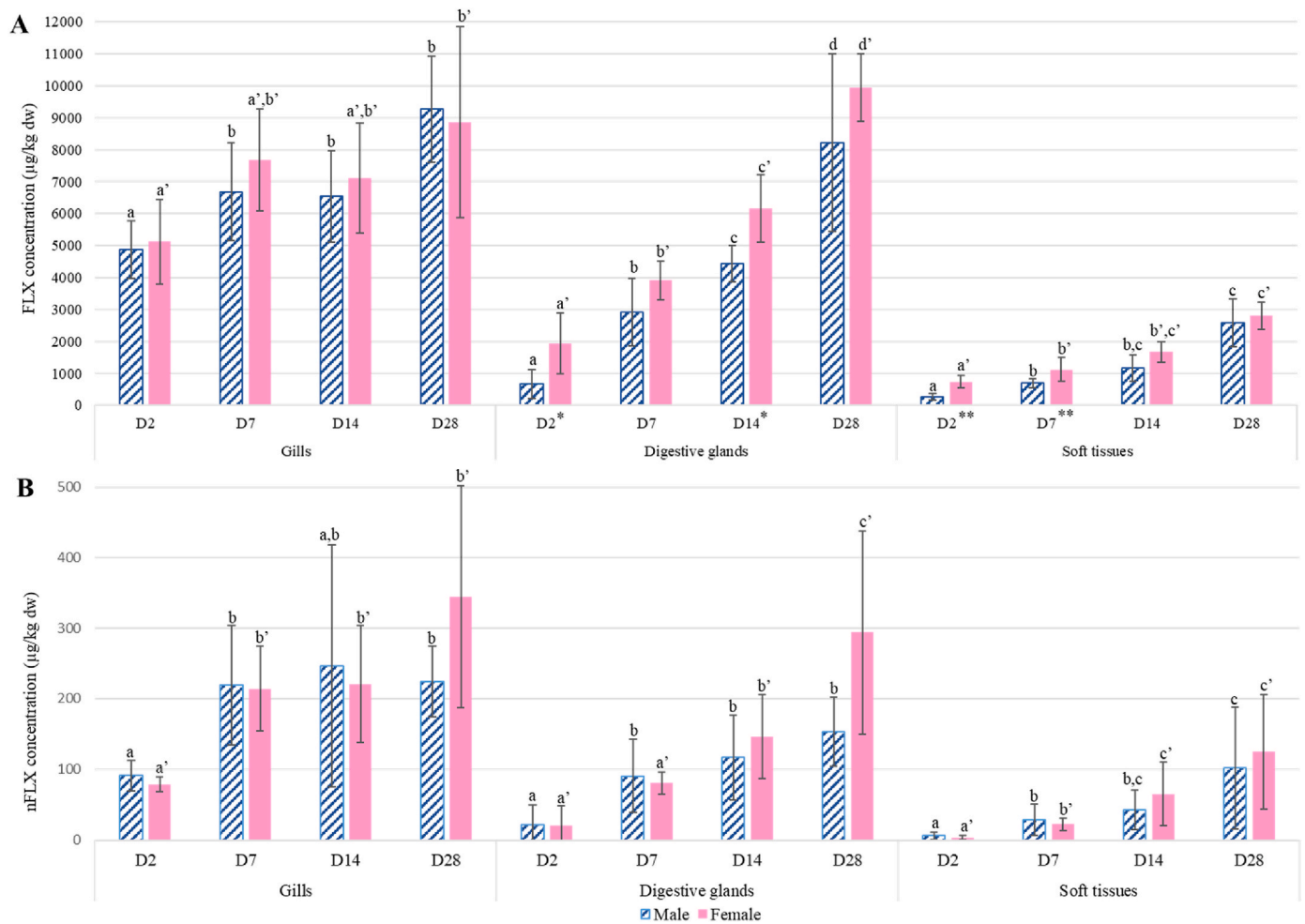


Fig. 3. (A) FLX and (B) NFLX concentration per tissues measured at four sampling times in male (n = 5) and female samples (n = 5). Hatched blue stands for male and pink for females. The different letters indicate significant differences ($p < 0.05$) between each sampling day (a, b, c and d for males and a', b', c' and d' for females). Significant difference between gender for a sampling time are reported at the bottom of the graphic (x-axis) by * $p < 0.05$; ** $p < 0.01$. (For interpretation of the references to colour in this figure legend, the reader is referred to the Web version of this article.)

The concentrations were higher in the gills than in the digestive glands and in the soft tissues. Regarding FLX in the gills, which are in direct contact with the exposure water, tissues concentrations were high from the first sampling time (D2) and increased slightly during the 28

days' exposure period with a significant increase between D2 and D7. No significant sex differences were observed between male and female in gills along the exposure period for both FLX and NFLX. Regarding both digestive glands and soft tissues, a regular increase in FLX and NFLX

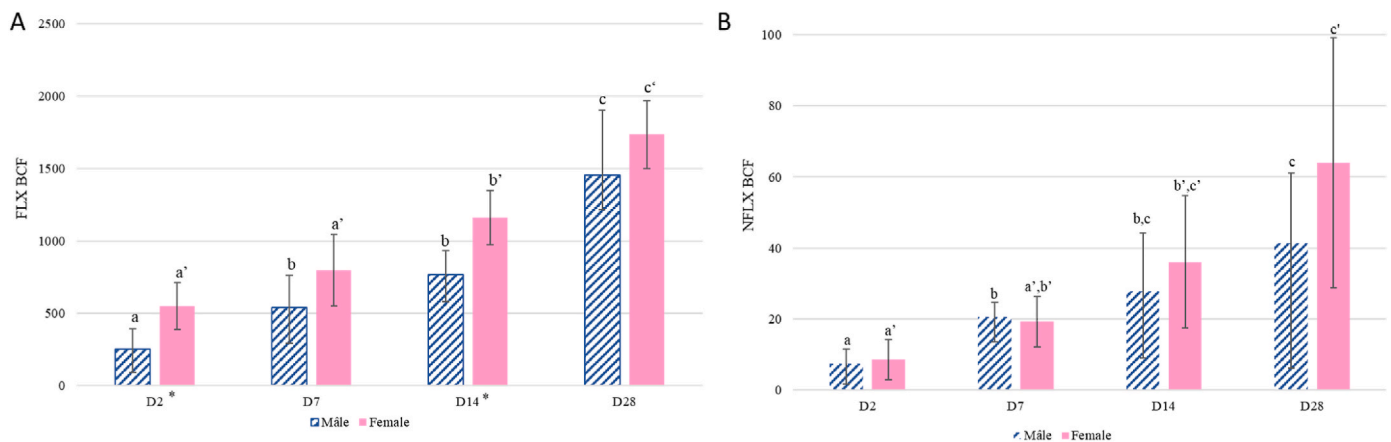


Fig. 4. (A) FLX BCF and (B) NFLX pseudo-BCF in mussel's whole body at four sampling times in male (n = 5) and female samples (n = 5). Hatched blue stands for male and pink for females. The different letters indicate significant differences ($p < 0.05$) between each sampling day (a, b and c for males and a', b' and c' for females). Significant difference between gender for a sampling time are reported at the bottom of the graphic (x-axis) by * $p < 0.05$. (For interpretation of the references to colour in this figure legend, the reader is referred to the Web version of this article.)

concentrations was observed across the various sampling days (more pronounced for FLX). Significant sex differences in FLX concentrations were observed on days 2 and 14 in digestive glands and on days 2 and 7 in soft tissues, with higher concentration in female in both case. Regarding NFLX, no significant differences between male and female were observed. Large error bars were observed for both FLX and NFLX concentrations, likely due to inter-individual differences in bioaccumulation and metabolism of FLX.

3.2.2. Bioconcentration of FLX and NFLX

The FLX BCF and NFLX pseudo-BCF were calculated on each sampling day (Fig. 4). All BCF and pseudo-BCF calculated at each sampling day for the three different organs are presented in Table S-1 and Table S-2.

The BCF values followed an increasing trend, similar to that observed for concentrations in digestive gland and soft tissues. For both male and female individuals, there was a significant increase over the exposure time of FLX BCF and NFLX pseudo-BCF. In the case of FLX, the BCF value increased from 253 at D2 to 1451 at D28 for males, and it increased from 551 at D2 to 1734 at D28 for females. Sex significant differences were observed on days 2 and 14. The pseudo-BCF of NFLX increased from 7 to 41 and from 9 to 64 and for males and females, respectively. Regarding NFLX pseudo-BCF, no significant difference between male and female was observed.

3.3. FLX biotransformation products

Eleven metabolites were highlighted through suspect-screening and non-targeted approaches and assigned numbers from M1 to M11 based on their increasing retention time (Table 2). Each metabolite was absent in the control samples. The retention times (with gradient optimized) of each metabolite are reported in Table 2. Extracted ion chromatograms (EIC) of FLX and its metabolites are provided for sampling day 28 in the Supplementary material along with an overlap chromatogram showing all metabolites in the retention time range (Figure S-3; Figure S-4). Abundances of each detected metabolite across the 4 sampling days are displayed in Figure S-5. and all MS² fragment spectra, along with proposed fragmentation mechanisms and structures are presented in Figure S-6 to Figure S-43. Similar increasing trends than FLX were observed for each metabolite with a maximum abundance at sampling day 28. On day 28, the most abundant area of metabolites in decreasing order was M8 > M6 > (M3+M4) > M9 > M8 > M5 > M11 > M1 > M2 > M10 (Figure S-5). N-Methyl-AcetoxyFLX was the most abundant metabolite, more abundant (hypothesizing similar ionization recovery in MS) than NFLX. A table with all documented metabolites in aquatic organisms (former studies and this study) was included in the supplementary data (Table S-3) for future LC-HRMS targeted analyses.

3.3.1. Target compound

FLX structure is represented with annotated carbons (Fig. 5). FLX was eluted at 4.41 min and its fragmentation mass spectrum revealed

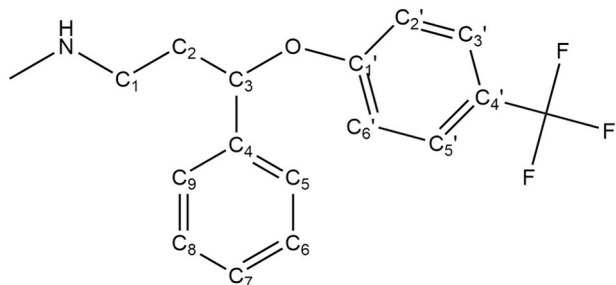


Fig. 5. FLX molecular formula with annotated carbons.

two main fragments (Figure S-6 to S-8). The first fragment, $[M+H]^+ = 148.1121$ corresponds to the elemental composition of $C_{10}H_{14}N$ and originates from a remote hydrogen rearrangement according to Demarque et al. resulting in the neutral loss liberation (Formula: $C_7H_5OF_3$ and exact mass: 162.0293) (Demarque et al., 2016). The other fragment was highlighted at m/z 117.0698 (C_9H_9 ; $\delta ppm = 0.91$) and corresponds to the first fragment with a simple inductive cleavage with charge migration and the loss of the primary amine group (Formula: CH_5N and exact mass 31.0422).

3.3.2. Phase 1 metabolites

3.3.2.1. Hydroxylation. Four metabolites, labeled M1, M2, M3 and M4 were detected at $[M+H]^+ = 326.1367$ in ESI+. They present a calculated mass shift of +15.9949 compared to FLX, characteristic of RH to ROH structure biotransformation, indicating the formation of hydroxyl metabolites. The difference in retention times (2.45, 3.06, 3.39 and 3.46 min) between the metabolites indicates that hydroxylation occurred at different positions on the parent compound. Shorter retention time compared to FLX aligns with the addition of an OH group, this addition increasing the polarity of the molecule, leading to earlier elution in reverse-phase LC.

M1, with a retention time of 2.45 min, presents 2 coherent fragments on the fragmentation spectrum (Figure S-9 to S-11) at m/z 164.1066, corresponding to the elemental composition of $C_{10}H_{14}NO$, after a remote hydrogen rearrangement with a neutral loss (Formula: $C_7H_5OF_3$ and exact mass: 162.0293) and at m/z 60.0447, corresponding to the elemental composition of C_2H_6NO , after hydrogen migration and a displacement reaction. These compositions allow with a good confidence the proposition of a chemical structure with an oxidation of the carbon next to nitrogen.

M2, with a retention time of 3.06 min, presents 2 coherent fragments on the fragmentation spectrum (Figure S-12 to S-14), at m/z 164.1067, corresponding to the elemental composition of $C_{10}H_{14}NO$, after a remote hydrogen rearrangement and a neutral loss (Formula: $C_7H_5OF_3$ and exact mass: 162.0293) and at m/z 117.0698, corresponding to the elemental composition of C_9H_9 , after a simple inductive cleavage with charge migration and the loss of the primary amine group bearing an oxidation (Formula: CH_5NO and exact mass 47.0371). These compositions allow with a good confidence to propose a chemical structure with an oxidation of the terminal carbon or on the nitrogen itself.

M3, with a retention time of 3.39 min, partially coeluted with M4, presents only one coherent fragment on the fragmentation spectrum (Figure S-15 to S-17), at m/z 164.1073, corresponding to the elemental composition of $C_{10}H_{14}NO$, after a remote hydrogen rearrangement with a neutral loss (Formula: $C_7H_5OF_3$ and exact mass: 162.0293). This composition allows only the proposition of a chemical structure with an oxidation somewhere on the left side, probably on the phenyl.

M4, with a retention time of 3.46 min presents only one coherent fragment on the fragmentation spectrum (Figure S-18 to S-20), at m/z 148.1118, corresponding to the elemental composition of $C_{10}H_{14}N$, after a remote hydrogen rearrangement with a neutral loss (Formula: $C_7H_5O_2F_3$ and exact mass: 178.0242). This composition allows the proposition of a chemical structure with an oxidation on the fluorinated part.

3.3.2.2. FLX hydrolysis. M5, with a retention time of 3.95 min, was detected only in ESI⁻ and exhibited $[M - H]^- = 161.0221$. This metabolite was attributed to the TFMP metabolite, which is formed primarily by the hydrolysis of C3-O bond of FLX (Figure S-21 to S-23). Only one fragment was observed: a loss of HF at m/z 141.0161. TFMP was identified with confidence level 1, supported by the availability of its analytical standard injected in the same analytical conditions.

3.3.2.3. N-demethylation. M6, with a retention time of 4.07 min, exhibited an exact mass of $[M+H]^+ = 296.1260$. The mass shift observed with FLX corresponds to a difference of CH_2 , indicating the formation of the NFLX metabolite through N-demethylation of FLX. A fragment was highlighted at m/z 134.0965, corresponding to an elemental composition of $C_9H_{12}N$, after a remote hydrogen rearrangement with a neutral loss (Formula: $C_7H_5OF_3$ and exact mass: 162.0293) (Figure S-24 to S-26). This metabolite was identified and confirmed at level 1 with an analytical standard injected under the same LC-MS conditions.

3.3.3. Phase II metabolites

3.3.3.1. N-methylation conjugation. M7, with a retention time of 4.67 min, was highlighted in ESI^+ at $[M+H]^+ = 324.1576$. M7 exhibited a calculated mass shift of +14.0156 compared to FLX. This mass difference can be associated with CH_2 corresponding to N-methylation of FLX. The fragmentation of the $[M+H]^+$ displayed two fragments at m/z 162.1276, corresponding to an elemental composition of $C_{11}H_{16}N$, after a remote hydrogen rearrangement with a neutral loss (Formula: $C_7H_5OF_3$ and exact mass: 162.0293), and at m/z 58.0651 (C_3H_8N) (Figure S-27 to S-29). These compositions allow the proposition of a chemical structure with a methylation on the amine part.

3.3.3.2. N-acylation conjugation. Three metabolites were detected after N-acylation with aldehydes in ESI^+ . M9, M10 and M11 were detected at m/z 338.1356, 352.1524 and 364.1528 respectively at retention time 6.74, 6.79 and 6.95 min.

The theoretical chemical formula of M9, attributed by XCalibur software for $[M+H]^+ = 338.1356$, was $C_{18}H_{18}F_3NO_2$ ($\delta ppm = 1.96$). After a remote hydrogen rearrangement with a neutral loss (Formula: $C_7H_5OF_3$ and exact mass: 162.0293), a fragment at m/z 176.1072 (compared to fragment at m/z 148.1123 for FLX) is formed corresponding to the addition of CO (+27.995) on FLX (Figure S-30 to S-32). To observe the fragment at m/z 117.0699, similar to FLX fragmentation, the modification is placed near the nitrogen and the protonation occurred on the nitrogen or the carbonyl of the formylation, this second option being more stable. In contrast, an interesting fragment is observed at m/z 72.0445 (C_3H_6NO) with the confirmation of the formylation, but certainly originating from the fragmentation of $[M+H]^+$, with the protonation on the ether group. Finally originating from the neutral 162.0293 losing an anion fluorine a stable cation structure is observed at m/z 143.0305. Based on these elements and the standard injection in the same LC-MS conditions, M10 was attributed to N-formylFLX at confidence level 1 formed by N-formylation of FLX.

Concerning M10 metabolite, a mass shift observed between $[M+H]^+ = 352.1524$ and FLX was +42.0106 corresponding to the addition of C_2H_2O on the parent compound. As described previously, after a remote hydrogen rearrangement with a neutral loss (Formula: $C_7H_5OF_3$ and exact mass: 162.0293), the fragment at m/z 190.1229 is formed corresponding to the elemental composition $C_{12}H_{16}NO$ (Figure S-33 to S-35). To observe the fragment at m/z 117.0697, the modification is placed near the nitrogen and the protonation occurred on the nitrogen or the carbonyl of the acetylation, this second option being more stable. In contrast, another fragment highlighted at m/z 86.0601 attributed to C_4H_8NO by Xcalibur software might be originated from a protonation on the ether group, with first an inductive cleavage and then a retro-ene reaction. Based on these elements the structure is certainly a FLX N-acetylation ($C_{19}H_{20}F_3NO_2$; $\delta ppm = 1.46$).

The third metabolite, M11, exhibited a mass shift of +54.0114. Annotation of this metabolite was guided by the literature and suggested its formation through N-acylation of FLX. M11 showed two characteristic fragments at m/z 202.1227 ($C_{13}H_{16}NO$) and m/z 98.0600 (C_5H_8NO) (Figure S-36 to S-38). This spectrum is interesting with the presence of a real C–O homolytic bond cleavage. The $[M+H]^+$ provides

a radical cation at m/z 203.1302 after the loss of a radical $C_7H_4OF_3$, like the pair m/z 202 and 98, the awaited m/z 99.0679 is also present and can provide the fragment at 82.0651 after the loss of a radical OH. The fragment at m/z 70.0653 is certainly a carbon monoxide elimination ($-CO$) from m/z 98.0600. The ion at m/z 202 provides also this $-CO$ at m/z 174.1275 and a $-CO-C_2H_2$ at m/z 146.0692. The ion at m/z 251.0682 is originated from the cleavage between the equivalent of C2 and C3.

3.3.3.3. Conjugation to fluoxetine phase I metabolites. M8 eluted at 4.69 min, presents an exact mass in ESI^+ of 382.1631 and in ESI^- of 380.1479, with a mass shift of +72.0217 compared to FLX. The attributed theoretical chemical formula of this compound was $C_{20}H_{22}F_3NO_3$ ($\delta ppm = 1.69$), suggesting possible modifications with a complete formula of $C_3H_5O_2$ in comparison to FLX. One fragment (C–O bond cleavage) detected in negative mode corresponds to the TFMP fragment at m/z 161.0218, confirming that there was no modification on the fluorinated part of the molecule (Figure S-39 to S-41). In positive mode, a fragment was observed at m/z 220.1328 ($C_{13}H_{18}NO_2$; $\delta ppm = 1.72$) corresponding to a methylation, an acetylation and a hydroxylation (Figure S-42 to S-44). The fragment at m/z 116.0703 ($C_5H_{10}NO_2$; $\delta ppm = 2.78$) resulted from the cleavage between C₁ and C₂. The fragment at 74.0601 (C_3H_8NO) is in agreement with an acetylation. An interesting fragment at m/z 322.1428 allows understanding that the acetylation is directly connected to an oxygen with a classical hydrogen remote rearrangement with a neutral loss of acetic acid (m/z 60.0211, $C_2H_4O_2$). With these elements, it is logical to assume a methylation on nitrogen, the structure is certainly the N-Methyl-AcetoxyFLX.

4. Discussion

4.1. Rapid uptake of FLX by mussels

FLX is known to be resistant to photolysis, hydrolysis, and microbial degradation (Kwon and Armbrust, 2006), which confirms the slight loss of fluoxetine observed in aquaria without mussels. In the presence of mussels, a rapid decrease in FLX concentration during exposure was reported in this study. This was particularly noticeable after water and FLX concentration renewal. Similar observations were reported in other studies. For instance, Hazelton et al. reported a significant and rapid depletion of FLX concentration from time 0–72 h post-treatment in experiments involving *L. fasciola* mussels. This was especially true for high concentrations of FLX (5 and 50 $\mu g/L$), where measured concentrations after spiking were 2.5 and 22.3 $\mu g/L$, respectively. (Hazelton et al., 2014). Lazzara et al. have exposed for 6 days *D. polymorpha* zebra mussels to two concentrations of FLX (20 and 200 ng/L). For the highest concentration, they observed that FLX levels in exposure water dropped at 110 ng/L after 24 h of exposure, suggesting uptake of the compound by the test organisms (Lazzara et al., 2012). These observations, along with our own, confirm that mussels filter, absorb, and accumulate FLX over time. This trend persisted throughout the entire exposure period in our study and was further confirmed by the quantification of FLX in the different tissues of the mussels.

A clear increase in FLX concentration was observed over time in the digestive gland and soft tissues. This increase was not as significant in the gills compared to the other tissues analyzed. A similar trend was observed with NFLX. Gills, as the organ in direct contact with the environment in marine invertebrates, may be the first to accumulate contaminants. The high FLX concentrations quantified in gills, from the onset of exposure, attested it. Subsequent detoxification processes, primarily occurring in the digestive gland, contributed to the accumulation of FLX and NFLX in this organ as well. Conversely, low concentrations in soft tissues suggested potential dilution or diffusion of both metabolized and non-metabolized FLX throughout the organism. This accumulation pattern is quite similar with previous research by Franzelitti et al. in

M. galloprovincialis. Their findings, after a 7-day exposure to FLX concentrations of 30 and 300 ng/L showed accumulation levels ordered as follows: digestive gland \geq gills > mantle/gonads while our results showed order gills > digestive gland > mantle/gonads at days 7 (Franzellitti et al., 2014). After 7 days of exposure, accumulation levels ordered as observed in the study of Franzellitti. In contrast to their study, where FLX administration was performed along with mussel feeding, our study involved feeding 1 h before FLX spike. FLX being known to bind strongly to particulate materials (e.g., over 50% (Baker and Kasprzyk-Hordern, 2011)), exposure in Franzellitti et al. study may have occurred likely through both water and trophic transfer, while our exposure was mainly conducted through water exposure. This may explain the differential accumulation patterns between gills and digestive glands observed at the beginning of the exposure.

Several FLX BCF and NFLX pseudo-BCF values are available in the literature, which are in line with the calculated BCF of this study (from 253 at D2 to 1734 at D28 for FLX, and from 7 at D2 to 64 at D28 for NFLX). In mussels, BCFs ranging from 200 to 800 were observed depending on the exposure concentrations (30 and 300 ng/L) and organs considered (digestive gland, gills and mantle/gonads) (Franzellitti et al., 2014). In another study, *Mytilus galloprovincialis*, exposed to a FLX concentration of 75 ng/L for 15 days, showed BCF values of 34, 59, and 124 at days 3, 7 and 15, respectively, along with pseudo-BCF values of 4, 38, and 155 (Silva et al., 2016). In *L. fasciola* mussels BCFs values of 509, 229, and 1221, were observed at FLX concentrations of 0.5, 5, and 50 $\mu\text{g/L}$ respectively after 67 days of exposure (Hazelton et al., 2014). Finally, the bioaccumulation of fluoxetine in the freshwater mussel *Elliptio complanata*, which were caged downstream of a municipal wastewater treatment facility effluent discharge resulted in BAFs ranging from 1250 to 1347 (Bringolf et al., 2010). Our BCF values are similar to those observed in other studies involving *Mytilus* exposed to FLX (Franzellitti et al., 2014; Hazelton et al., 2014). Semi-static

experiment was conducted in all 3 studies, despite differences in target nominal concentrations and exposure times, which did not result in significant BCF differences. Silva et al. reported lower BCF values compared to other studies. They concluded that the steady state was not reached and would only be achieved after 52 days of exposure under their conditions, which included no feeding of the mussels throughout the experiment (a divergence from other studies). We can therefore conclude that the steady state was likely reached in our study, even if the low pseudo-BCF of NFLX appears surprising. Indeed, throughout the experiment, the NFLX to FLX ratio of our study remained consistently below 1 (average of 0.03) indicating that FLX accumulation outpaced metabolism. A similar trend was observed in Silva et al. (2016), where *M. galloprovincialis* was exposed to a FLX concentration of 75 ng/L for 15 days. During the initial week of exposure, NFLX to FLX ratios of 0.12 and 0.64 were observed at days 3 and 7, respectively. However, by the end of the exposure period, this trend reversed, with an NFLX to FLX ratio of 1.25 on day 15. Other studies (in fish) have shown that the NFLX to FLX ratio fluctuates based on the concentration of exposure. At low and moderate concentrations, the ratio surpassed 1, whereas at high concentrations, the ratio fell below or around 1. These concentration thresholds vary according to the species under investigation (e.g., 30 and 300 ng/L in Japanese medaka; 50 and 5000 $\mu\text{g/L}$ in zebrafish) (Zindler et al., 2020; Nakamura et al., 2008). It has been shown in humans that FLX can inhibit FLX-metabolizing enzymes (Jeppesen et al., 1996; Stokes and Holtz, 1997; Mandrioli et al., 2006). If the same observation was true for aquatic organisms, impaired biotransformation processes could limit the metabolism of FLX and explain our low pseudo-BCF for NFLX.

During the experiment, significant differences in FLX accumulation between males and females were observed in both the digestive gland and soft tissues. However, these differences were no longer observable after 28 days of exposure. The different accumulation between male and

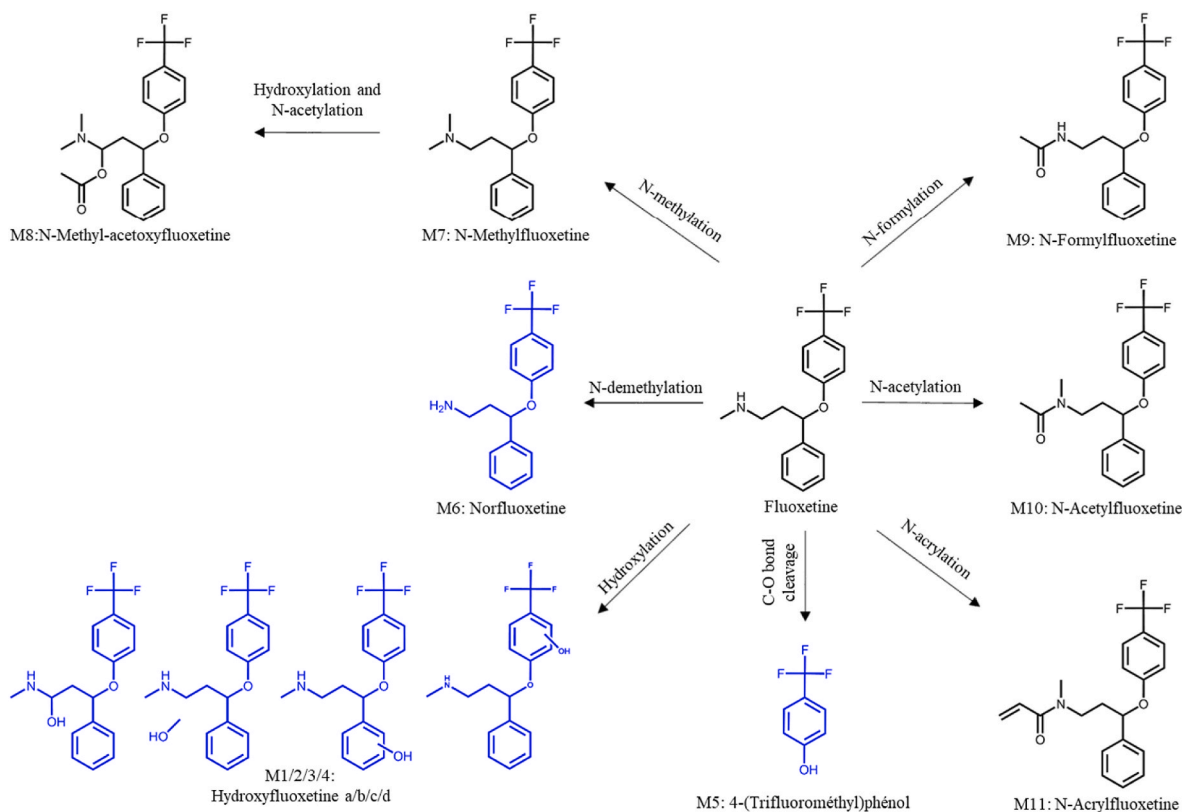


Fig. 6. Scheme depicting the formation of FLX metabolites following exposure to FLX. (Phase I metabolites in blue, Phase II metabolites in black.) Based on confidence level according to Shimanski et al. (2014), level 1: M5, M6 and M9; level 2a: M2, M7, M10 and M11; level 2b: M1, M3, M4 and M8. (For interpretation of the references to colour in this figure legend, the reader is referred to the Web version of this article.)

female of hydrophobic organic contaminants, such as FLX (log Kow = 4.05) (Oakes et al., 2010), could be influenced by lipid composition. A positive correlation has been observed between accumulation of these contaminants and the triglyceride content in mussels (*G. demissa*) (Bergen et al., 2001). Additionally, difference in fatty acid composition in *Mytilus galloprovincialis* between male and female were highlighted by Fernández-Reiriz et al. (2015), which could explain different FLX bioaccumulation between sexes. However, this analysis was not conducted in the present study.

4.2. FLX products of biotransformation

Non-targeted analysis of mussels' digestive gland enabled to highlight six Phase I metabolites and five Phase II metabolites. Fig. 6 is a schematic representation depicting the formation of metabolites along with proposed molecular structures. The presence of NFLX was not surprising since it has already been reported several times across various organisms, such as *Mytilus* (Silva et al., 2016). In this study, ten other metabolites of FLX were observed. Contrary to the expectations and assuming similar ionization recoveries, NFLX was not the predominant metabolite as documented in human studies (Mandrioli et al., 2006; Margolis et al., 2000; Deodhar et al., 2021). Instead, N-Methyl-AcetoxyFLX emerged as the predominant metabolite.

In *M. galloprovincialis* the presence of cytochrome P450 have already been highlighted and reported to favor enzymatic reactions involved in the metabolism of pharmaceuticals (Snyder, 2000; Bebianno et al., 2007). Four Phase I metabolites involving hydroxylation of FLX have been previously reported in other studies, although not in *Mytilus* spp. (Tisler et al., 2019; Zindler et al., 2020; Yan et al., 2023). The hydroxyl group position was discussed by Tisler et al. (2019), who observed hydroxylation on the benzyl group to form a phenol and on nitrogen heteroatom, as evidenced in this study (probably M2). Additionally, two hydroxyl metabolites were reported with confidence for the first time based on MS2 spectra structure elucidation. The first metabolite showed hydroxylation of the carbon next to the nitrogen, while the second metabolite exhibited hydroxylation on the fluorinated moiety. It is possible that hydroxylation may take place in different positions depending on the species. In mussels' organism, the hydroxylation process has already been observed in laboratory exposure to venlafaxine (Ariza-Castro et al., 2021). This hydroxylation process is associated with the detoxification pathway and is often followed by conjugation (Sathishkumar et al., 2020), which we observed in this study with N-Methyl-AcetoxyFLX (M8). The N-demethylation process leads to the formation of NFLX metabolite in *Mytilus*, as previously observed in laboratory-exposed mussels with venlafaxine (Ariza-Castro et al., 2021). This behavior is consistent with the mussel detoxification process, where the aim is to produce more hydrophilic metabolites, thereby facilitating their excretion. The formation of NFLX has been reported in several studies across various organisms, such as crabs and mussels (Silva et al., 2016; Robert et al., 2017). TFMP metabolite has already been observed in human plasma and urine and in rat urine and tissues (Urichuk et al., 1997). Regarding aquatic organisms, studies have reported its formation in microalgae (Xie et al., 2022) and in zebrafish embryos exposed to FLX (Tisler et al., 2019; Zindler et al., 2020).

All phase II metabolites formed by N-alkylation (N-methylation) and N-acylation conjugation (N-formylation, N-acetylation and N-acrylation) were previously described in studies involving zebrafish embryos (Tisler et al., 2019; Zindler et al., 2020), except M8 (N-Methyl-AcetoxyFLX). N-methylation process is conducted by N-methyl-transferase. N-methylation has already been observed as a contaminant detoxification process in mussels for o-toluidine, an organic compound used as an intermediate in the dye industry (Knezovich and Crosby, 1985). N-formylation of FLX has also been observed in microalgae (Xie et al., 2022)

and this process of N-formylation has already been observed in mussels for o-toluidine (Knezovich and Crosby, 1985). However, to our knowledge, N-acetylation and N-acrylation have never been documented as a contaminant detoxification process in *Mytilus*. Concerning N-methylation associated with hydroxylation followed by O-acetylation, this hypothesis has not been confirmed by the literature, as this metabolite is being reported for the first time. As N-acetylation and N-acrylation, O-acetylation process has never been observed in mussels as a biotransformation process.

N-succinylation and N-acylation with L-valine were not observed in this study in contrast with observation in zebrafish embryos and microalgae (Tisler et al., 2019; Zindler et al., 2020; Xie et al., 2022). This could possibly be explained by the fact that mussels are not capable of producing such metabolites, since N-succinylation or N-acylation with valine has never been observed for any contaminants in *Mytilus* spp. even though conjugation with leucine has been reported for diclofenac (Bonfille et al., 2017). A second hypothesis could be that the analytical protocol conducted in this study is not suited for these compounds meaning that the sample preparation method may not facilitate their retention or alternatively, that the concentration of these compounds may fall below the detection limit.

5. Conclusion

The application of targeted and non-targeted approaches proved effective in investigating FLX bioaccumulation and biotransformation products in *M. galloprovincialis*. A significant accumulation of the parent compound was observed over time along with the detection of eleven metabolites (6 phase I and 5 phase II). Notably, this study highlighted two phase I metabolites and one phase II metabolite previously unreported. Additionally, it is the first time that metabolites other than NFLX are reported in *Mytilus* spp. These findings contribute to the understanding of FLX metabolism in *Mytilus* and enhance the knowledge of pharmaceuticals detoxification processes in non-target organisms.

Declaration of generative AI in scientific writing

During the preparation of this work the author(s) used ChatGPT in order to improve the readability and language of the manuscript. After using this tool/service, the author(s) reviewed and edited the content as needed and take(s) full responsibility for the content of the published article.

CRediT authorship contribution statement

E. Lemaire: Writing – original draft, Visualization, Validation, Methodology, Formal analysis, Conceptualization. **E. Gomez:** Writing – review & editing, Project administration, Conceptualization. **N. Le Yondre:** Writing – review & editing, Formal analysis. **A. Malherbe:** Methodology. **F. Courant:** Writing – review & editing, Project administration, Methodology, Conceptualization.

Declaration of competing interest

The authors declare that they have no known competing financial interests or personal relationships that could have appeared to influence the work reported in this paper.

Data availability

Data will be made available on request.

Acknowledgment

The doctoral grant of Etienne Lemaire was financially supported by the Agence nationale de sécurité sanitaire, de l'alimentation, de l'environnement et du travail (ANSES-21-EST-072). The authors thank the Platform of Non-Target Environmental Metabolomics (PONTEM) of the consortium facilities Montpellier Alliance for Metabolomics and Metabolism Analysis (MAMMA).

Appendix A. Supplementary data

Supplementary data to this article can be found online at <https://doi.org/10.1016/j.chemosphere.2024.143314>.

References

- Afsa, S., Hamden, K., Lara Martin, P.A., Mansour, H.B., 2020. Occurrence of 40 pharmaceutically active compounds in hospital and urban wastewaters and their contribution to Mahdia coastal seawater contamination. *Environ. Sci. Pollut. Res.* 27, 1941–1955. <https://doi.org/10.1007/s11356-019-06866-5>.
- Ariza-Castro, N., Courant, F., Dumas, T., Marion, B., Fenet, H., Gomez, E., 2021. Elucidating venlafaxine metabolism in the Mediterranean mussel (*Mytilus galloprovincialis*) through combined targeted and non-targeted approaches. *Sci. Total Environ.* 779, 146387. <https://doi.org/10.1016/j.scitotenv.2021.146387>.
- Baker, D.R., Kasprzyk-Hordern, B., 2011. Multi-residue determination of the sorption of illicit drugs and pharmaceuticals to wastewater suspended particulate matter using pressurised liquid extraction, solid phase extraction and liquid chromatography coupled with tandem mass spectrometry. *J. Chromatogr. A* 1218, 7901–7913. <https://doi.org/10.1016/j.chroma.2011.08.092>.
- Bebiano, M.J., Lopes, B., Guerra, L., Hoarau, P., Ferreira, A.M., 2007. Glutathione S-transferases and cytochrome P450 activities in *Mytilus galloprovincialis* from the South coast of Portugal: effect of abiotic factors. *Environ. Int.* 33, 550–558. <https://doi.org/10.1016/j.envint.2006.11.002>.
- Bergen, B.J., Nelson, W.G., Quinn, J.G., Jayaraman, S., 2001. Relationships among total lipid, lipid classes, and polychlorinated biphenyl concentrations in two indigenous populations of ribbed mussels (*Geukensia demissa*) over an annual cycle. *Environ. Toxicol. Chem.* 20, 575–581. <https://doi.org/10.1002/etc.5620200317>.
- Biel-Maeso, M., Baena-Nogueras, R.M., Corada-Fernández, C., Lara-Martín, P.A., 2018. Occurrence, distribution and environmental risk of pharmaceutically active compounds (PhACs) in coastal and ocean waters from the Gulf of Cadiz (SW Spain). *Sci. Total Environ.* 612, 649–659. <https://doi.org/10.1016/j.scitotenv.2017.08.279>.
- Birch, G.F., Drage, D.S., Thompson, K., Eaglesham, G., Mueller, J.F., 2015. Emerging contaminants (pharmaceuticals, personal care products, a food additive and pesticides) in waters of Sydney estuary, Australia. *Mar. Pollut. Bull.* 97, 56–66. <https://doi.org/10.1016/j.marpolbul.2015.06.038>.
- Boeing, D.W., 1999. An evaluation of bivalves as biomonitors of heavy metals pollution in marine waters. *Environ. Monit. Assess.* 55, 459–470. <https://doi.org/10.1023/A:1005995217901>.
- Bonnefille, B., Arpin-Pont, L., Gomez, E., Fenet, H., Courant, F., 2017. Metabolic profiling identification of metabolites formed in Mediterranean mussels (*Mytilus galloprovincialis*) after diclofenac exposure. *Sci. Total Environ.* 583, 257–268. <https://doi.org/10.1016/j.scitotenv.2017.01.063>.
- Boxall, A.B.A., Rudd, M.A., Brooks, B.W., Caldwell, D.J., Choi, K., Hickmann, S., Innes, E., Ostapyk, K., Staveley, J.P., Verslycke, T., Ankley, G.T., Beazley, K.F., Belanger, S.E., Berninger, J.P., Carriquiriborde, P., Coors, A., DeLeo, P.C., Dyer, S.D., Ericson, J.F., Gagné, F., Giesy, J.P., Gouin, T., Hallstrom, L., Karlsson, M.V., Larsson, D.G.J., Lazorchak, J.M., Mastrocco, F., McLaughlin, A., McMaster, M.E., Meyerhoff, R.D., Moore, R., Parrott, J.L., Snape, J.R., Murray-Smith, R., Servos, M.R., Sibley, P.K., Straub, J.O., Szabo, N.D., Topp, E., Tetreault, G.R., Trudeau, V.L., Van Der Kraak, G., 2012. Pharmaceuticals and personal care products in the environment: what are the big questions? *Environ. Health Perspect.* 120, 1221–1229. <https://doi.org/10.1289/ehp.1104477>.
- Bringolf, R.B., Heltsley, R.M., Newton, T.J., Eads, C.B., Fraley, S.J., Shea, D., Cope, W.G., 2010. Environmental occurrence and reproductive effects of the pharmaceutical fluoxetine in native freshwater mussels. *Environ Toxicol Chem n/a-n/a*. <https://doi.org/10.1002/etc.157>.
- Claesson, A., Svensson, U., 1996. *Läkemedelskemi, second ed.* Apotekarsocieteten.
- Cranford, P.J., Ward, J.E., Shumway, S.E., 2011. Bivalve filter feeding: variability and limits of the aquaculture biofilter. In: *Shumway, S.E. (Ed.), Shellfish Aquaculture and the Environment, first ed.* Wiley, pp. 81–124.
- Demarque, D.P., Crotti, A.E.M., Vescechi, R., Lopes, J.L.C., Lopes, N.P., 2016. Fragmentation reactions using electrospray ionization mass spectrometry: an important tool for the structural elucidation and characterization of synthetic and natural products. *Nat. Prod. Rep.* 33, 432–455. <https://doi.org/10.1039/C5NP00073D>.
- Deodhar, M., Rihani, S.B.A., Darakjian, L., Turgeon, J., Michaud, V., 2021. Assessing the mechanism of fluoxetine-mediated CYP2D6 inhibition. *Pharmaceutics* 13, 148. <https://doi.org/10.3390/pharmaceutics13020148>.
- Diaz-Camal, N., Cardoso-Vera, J.D., Islas-Flores, H., Gómez-Oliván, L.M., Mejía-García, A., 2022. Consumption and occurrence of antidepressants (SSRIs) in pre- and post-COVID-19 pandemic, their environmental impact and innovative removal methods: a review. *Sci. Total Environ.* 829, 154656. <https://doi.org/10.1016/j.scitotenv.2022.154656>.
- Fernández-Reiriz, M., Garrido, J., Irisarri, J., 2015. Fatty acid composition in *Mytilus galloprovincialis* organs: trophic interactions, sexual differences and differential anatomical distribution. *Mar. Ecol. Prog. Ser.* 528, 221–234. <https://doi.org/10.3354/meps11280>.
- Fong, P.P., Ducan, J., Ram, J.L., 1994. Inhibition and sex specific induction of spawning by serotonergic ligands in the zebra mussel *Dreissena polymorpha* (Pallas). *Experientia* 50, 506–509. <https://doi.org/10.1007/BF01920759>.
- Franzellitti, S., Buratti, S., Capolupo, M., Du, B., Haddad, S.P., Chambliss, C.K., Brooks, B.W., Fabbri, E., 2014. An exploratory investigation of various modes of action and potential adverse outcomes of fluoxetine in marine mussels. *Aquat. Toxicol.* 151, 14–26. <https://doi.org/10.1016/j.aquatox.2013.11.016>.
- Gaitán-Espitia, J.D., Quintero-Galvis, J.F., Mesas, A., D'Elía, G., 2016. Mitogenomics of southern hemisphere blue mussels (*Bivalvia*: pteriomorpha): insights into the evolutionary characteristics of the *Mytilus edulis* complex. *Sci. Rep.* 6, 26853. <https://doi.org/10.1038/srep26853>.
- Hazelton, P.D., Du, B., Haddad, S.P., Fritts, A.K., Chambliss, C.K., Brooks, B.W., Bringolf, R.B., 2014. Chronic fluoxetine exposure alters movement and burrowing in adult freshwater mussels. *Aquat. Toxicol.* 151, 27–35. <https://doi.org/10.1016/j.aquatox.2013.12.019>.
- Holman, J.D., Tabb, D.L., Mallick, P., 2014. Employing ProteoWizard to convert raw mass spectrometry data. *Current Protocols in Bioinformatics* 46, 13.24.1–13.24.9. <https://doi.org/10.1002/0471250953.bi1324s46>.
- Jeppesen, U., Gram, L.F., Vistisen, K., Loft, S., Poulsen, H.E., Brøsen, K., 1996. Dose-dependent inhibition of CYP1A2, CYP2C19 and CYP2D6 by citalopram, fluoxetine, fluvoxamine and paroxetine. *Eur. J. Clin. Pharmacol.* 51, 73–78. <https://doi.org/10.1007/s002280050163>.
- Knezovich, J.P., Crosby, D.G., 1985. Fate and metabolism of *o*-toluidine in the marine bivalve molluscs *Mytilus edulis* and *Crossostrea gigas*. *Environ. Toxicol. Chem.* 4, 435–446. <https://doi.org/10.1002/etc.5620040403>.
- Kwon, J.-W., Armbrust, K.L., 2006. Laboratory persistence and fate of fluoxetine in aquatic environments. *Environ. Toxicol. Chem.* 25 (1), 2561–2568. <https://doi.org/10.1897/05-613R>.
- Lazzara, R., Blázquez, M., Porte, C., Barata, C., 2012. Low environmental levels of fluoxetine induce spawning and changes in endogenous estradiol levels in the zebra mussel *Dreissena polymorpha*. *Aquat. Toxicol.* 106–107, 123–130. <https://doi.org/10.1016/j.aquatox.2011.11.003>.
- Mandrioli, R., Forti, G., Raggi, M., 2006. Fluoxetine metabolism and pharmacological interactions: the role of cytochrome P450. *CDM* 7, 127–133. <https://doi.org/10.2174/138920006775541561>.
- Margolis, J.M., O'Donnell, J.P., Mankowski, D.C., Ekins, S., Obach, R.S., 2000. (R)-, (S)-, and racemic fluoxetine N-demethylation by human cytochrome P450 enzymes. *Drug Metab. Dispos.* 28, 1187–1191.
- Maruya, K.A., Vidal-Dorsch, D.E., Bay, S.M., Kwon, J.W., Xia, K., Armbrust, K.L., 2012. Organic contaminants of emerging concern in sediments and flatfish collected near outfalls discharging treated wastewater effluent to the Southern California Bight. *Environ. Toxicol. Chem.* 31, 2683–2688. <https://doi.org/10.1002/etc.2003>.
- Nakamura, Y., Yamamoto, H., Sekizawa, J., Kondo, T., Hirai, N., Tatarazako, N., 2008. The effects of pH on fluoxetine in Japanese medaka (*Oryzias latipes*): acute toxicity in fish larvae and bioaccumulation in juvenile fish. *Chemosphere* 70, 865–873. <https://doi.org/10.1016/j.chemosphere.2007.06.089>.
- Nödler, K., Voutsas, D., Licha, T., 2014. Polar organic micropollutants in the coastal environment of different marine systems. *Mar. Pollut. Bull.* 85, 50–59. <https://doi.org/10.1016/j.marpolbul.2014.06.024>.
- Oakes, K.D., Coors, A., Escher, B.I., Fenner, K., Garric, J., Gust, M., Knacker, T., Küster, A., Kussatz, C., Metcalfe, C.D., Monteiro, S., Moon, T.W., Mennigen, J.A., Parrott, J., Péry, A.R., Ramil, M., Roennefahrt, I., Tarazona, J.V., Sánchez-Argüello, P., Ternes, T.A., Trudeau, V.L., Boucard, T., Van Der Kraak, G.J., Servos, M.R., 2010. Environmental risk assessment for the serotonin re-uptake inhibitor fluoxetine: case study using the European risk assessment framework. *Integr. Environ. Assess. Manag.* 6, 524–539. <https://doi.org/10.1002/ieam.77>.
- OECD, 2019. *Pharmaceutical consumption*. In: *Health at a Glance 2019: OECD Indicators*. OECD Publishing, Paris. <https://doi.org/10.1787/43146d4b-en>.
- Paterson, G., Metcalfe, C.D., 2008. Uptake and depuration of the anti-depressant fluoxetine by the Japanese medaka (*Oryzias latipes*). *Chemosphere* 74, 125–130. <https://doi.org/10.1016/j.chemosphere.2008.08.022>.
- Regoli, F., Principato, G., 1995. Glutathione, glutathione-dependent and antioxidant enzymes in mussel, *Mytilus galloprovincialis*, exposed to metals under field and laboratory conditions: implications for the use of biochemical biomarkers. *Aquat. Toxicol.* 31, 143–164. [https://doi.org/10.1016/0166-445X\(94\)00064-W](https://doi.org/10.1016/0166-445X(94)00064-W).
- Reis-Santos, P., Pais, M., Duarte, B., Caçador, I., Freitas, A., Vila Pouca, A.S., Barbosa, J., Leston, S., Rosa, J., Ramos, F., Cabral, H.N., Gillanders, B.M., Fonseca, V.F., 2018. Screening of human and veterinary pharmaceuticals in estuarine waters: a baseline assessment for the Tejo estuary. *Mar. Pollut. Bull.* 135, 1079–1084. <https://doi.org/10.1016/j.marpolbul.2018.08.036>.
- Rizzi, C., Seveso, D., Galli, P., Villa, S., 2020. First record of emerging contaminants in sponges of an inhabited island in the Maldives. *Mar. Pollut. Bull.* 156, 111273. <https://doi.org/10.1016/j.marpolbul.2020.111273>.
- Robert, A., Schultz, I.R., Hucher, N., Monsinjon, T., Knigge, T., 2017. Toxicokinetics, disposition and metabolism of fluoxetine in crabs. *Chemosphere* 186, 958–967. <https://doi.org/10.1016/j.chemosphere.2017.08.018>.
- Sathishkumar, P., Meena, R.A.A., Palanisami, T., Ashokkumar, V., Palvannan, T., Gu, F. L., 2020. Occurrence, interactive effects and ecological risk of diclofenac in environmental compartments and biota - a review. *Sci. Total Environ.* 698, 134057. <https://doi.org/10.1016/j.scitotenv.2019.134057>.

- Schymanski, E.L., Jeon, J., Gulde, R., Fenner, K., Ruff, M., Singer, H.P., Hollender, J., 2014. Identifying small molecules via high resolution mass spectrometry: communicating confidence. *Environ. Sci. Technol.* 48, 2097–2098. <https://doi.org/10.1021/es5002105>.
- Silva, L.J.G., Pereira, A.M.P.T., Meisel, L.M., Lino, C.M., Pena, A., 2015. Reviewing the serotonin reuptake inhibitors (SSRIs) footprint in the aquatic biota: uptake, bioaccumulation and ecotoxicology. *Environ. Pollut.* 197, 127–143. <https://doi.org/10.1016/j.envpol.2014.12.002>.
- Silva, L.J.G., Martins, M.C., Pereira, A.M.P.T., Meisel, L.M., Gonzalez-Rey, M., Bebianno, M.J., Lino, C.M., Pena, A., 2016. Uptake, accumulation and metabolization of the antidepressant fluoxetine by *Mytilus galloprovincialis*. *Environ. Pollut.* 213, 432–437. <https://doi.org/10.1016/j.envpol.2016.02.022>.
- Silva, L.J.G., Pereira, A.M.P.T., Rodrigues, H., Meisel, L.M., Lino, C.M., Pena, A., 2017. SSRIs antidepressants in marine mussels from Atlantic coastal areas and human risk assessment. *Sci. Total Environ.* 603–604, 118–125. <https://doi.org/10.1016/j.scitotenv.2017.06.076>.
- Smith, C.A., Want, E.J., O'Maille, G., Abagyan, R., Siuzdak, G., 2006. XCMS: processing mass spectrometry data for metabolite profiling using nonlinear peak alignment, matching, and identification. *Anal. Chem.* 78, 779–787. <https://doi.org/10.1021/ac051437y>.
- Snyder, M.J., 2000. Cytochrome P450 enzymes in aquatic invertebrates: recent advances and future directions. *Aquat. Toxicol.* 48, 529–547. [https://doi.org/10.1016/S0166-445X\(00\)00085-0](https://doi.org/10.1016/S0166-445X(00)00085-0).
- Stokes, P.E., Holtz, A., 1997. Fluoxetine tenth anniversary update: the progress continues. *Clin. Therapeut.* 19, 1135–1250. [https://doi.org/10.1016/S0149-2918\(97\)80066-5](https://doi.org/10.1016/S0149-2918(97)80066-5).
- Tisler, S., Zindler, F., Freeling, F., Nödler, K., Toelgyesi, L., Braunbeck, T., Zwiener, C., 2019. Transformation products of fluoxetine formed by photodegradation in water and biodegradation in zebrafish embryos (*Danio rerio*). *Environ. Sci. Technol.* 53, 7400–7409. <https://doi.org/10.1021/acs.est.9b00789>.
- Urichuk, L.J., Aspeslet, L.J., Holt, A., Silverstone, P.H., Coutts, R.T., Baker, G.B., 1997. Determination of p-trifluoromethylphenol, a metabolite of fluoxetine, in tissues and body fluids using an electron-capture gas chromatographic procedure. *J. Chromatogr. B Biomed. Sci. Appl.* 698, 103–109. [https://doi.org/10.1016/S0378-4347\(97\)00304-6](https://doi.org/10.1016/S0378-4347(97)00304-6).
- Verlicchi, P., Al Aukidy, M., Zambello, E., 2012. Occurrence of pharmaceutical compounds in urban wastewater: removal, mass load and environmental risk after a secondary treatment—a review. *Sci. Total Environ.* 429, 123–155. <https://doi.org/10.1016/j.scitotenv.2012.04.028>.
- Xie, Z., Wang, X., Gan, Y., Cheng, H., Fan, S., Li, X., Tang, J., 2022. Ecotoxicological effects of the antidepressant fluoxetine and its removal by the typical freshwater microalgae *Chlorella pyrenoidosa*. *Ecotoxicol. Environ. Saf.* 244, 114045. <https://doi.org/10.1016/j.ecoenv.2022.114045>.
- Yan, Z., Chen, Y., Zhang, X., Lu, G., 2023. The metabolites could not be ignored: a comparative study of the metabolite norfluoxetine with its parent fluoxetine on zebrafish (*Danio rerio*). *Aquat. Toxicol.* 257, 106467. <https://doi.org/10.1016/j.aquatox.2023.106467>.
- Zindler, F., Tisler, S., Loerracher, A.-K., Zwiener, C., Braunbeck, T., 2020. Norfluoxetine is the only metabolite of fluoxetine in zebrafish (*Danio rerio*) embryos that accumulates at environmentally relevant exposure scenarios. *Environ. Sci. Technol.* 54, 4200–4209. <https://doi.org/10.1021/acs.est.9b07618>.